

First-principles Calculations on Co-segregation of P and Transition Metal Elements at Fe Grain Boundaries

Shinya MORITA*¹

*¹ Applied Physics Research Laboratory, Technical Development Group

Abstract

The first-principles (ab-initio) calculations based on the FeΣ3 (111) grain boundary model have been used to study the effects of transition metal elements, Cr, Mn, and Mo, on the grain-boundary co-segregation and of P contained in the steel and on the grain-boundary embrittlement. It has been found that Cr, Mn, and Mo indicate repulsive interactions with P at the grain boundaries of Fe and that the shorter the distance to the P atom, the stronger the repulsive interactions become. The interactions have turned out to be small relative to the grain boundary segregation energy of P, causing only a small effect on the segregation behavior of P. However, Mo, when segregated on the grain boundaries, increases the binding energy of the grain boundaries, and is expected to suppress the grain-boundary embrittlement due to P.

Introduction

In ferrous materials, grain boundaries are prone to brittle fracture. In particular, grain boundary embrittlement is well-known to occur when impurity elements such as P and S segregate on the grain boundary, decreasing material strength and ductility. Embrittlement phenomena due to grain boundary segregation include the low-temperature temper embrittlement of low alloy steel,¹⁾ grain boundary cracking by S segregation of Ni steel,²⁾ and high-temperature cracking in welding.³⁾ Controlling grain boundary segregation is an essential issue in various materials for mechanical structures.

In order to suppress grain boundary embrittlement, it is necessary not only to reduce grain boundary embrittlement elements such as P and S in steel to the utmost limit, but also to consider the influence of additive elements in the steel. For example, Mn has a high affinity with P and promotes co-segregation. In addition, Cr and Mo form carbide, reducing the grain-boundary segregation of C and promoting the segregation of P. Thus, alloying elements affect the segregation of P on grain boundaries due to various factors.

A certain amount of Mo has been reported to strengthen the grain boundaries while lowering the ductile-to-brittle transition temperature (DBTT).⁴⁻⁷⁾ When multiple elements segregate on grain boundaries, the amount of grain-boundary segregation may be affected by site competition for

stable sites (atomic positions) and by interatomic interaction. In reality, however, P, S, and transition metal elements in steel form carbides and alloy compounds, affecting the amount of solid solution that contributes to the grain boundary segregation. Therefore, it is difficult to quantitatively consider the effect of interatomic interaction on the grain boundary segregation of embrittling elements such as P and S.

On the other hand, the first-principles calculations allow the analysis of interatomic interactions, enabling the consideration of the mechanisms for grain boundary co-segregation. As a result, guidelines will be obtained for the future development of high-strength materials. Studies on grain boundary segregation, using first-principles calculations, have also been conducted on ferrous materials. Its effects on segregation tendency and grain boundary strength are considered using indexes such as grain boundary segregation energy and grain boundary binding energy.⁸⁾⁻¹⁰⁾ For example, Yamaguchi et al. studied the grain boundary segregation of light elements such as P using the Σ3 (111) grain boundary of bcc iron as a model. They clarified that the grain boundary aggregation energy correlates with the ductile-to-brittle transition temperature.⁸⁾

However, no report considers the co-segregation of P with transition metal elements in actual materials. Therefore, this study uses first-principles calculations to investigate the effects of transition metal elements, Cr, Mn, and Mo, on the grain boundary segregation of P and the grain boundary strength, these being elements that are widely used to strengthen ferrous materials, for example.

1. Calculation method

The first-principles calculations for the grain boundaries have employed the bcc-Fe Σ3 (111) grain-boundary model (76 atoms) with excellent symmetry. **Fig. 1** shows the grain-boundary model. Here, the central part is the grain boundary, the upper and lower surface sides are provided with vacuum layers, and all three axes are periodic boundary conditions. The grain boundary energy calculated on the basis of this model is 1.23 J/m², which is close to the energy value, 1.48 J/m²,¹¹⁾ of Σ27 (552) grain boundary, an almost random

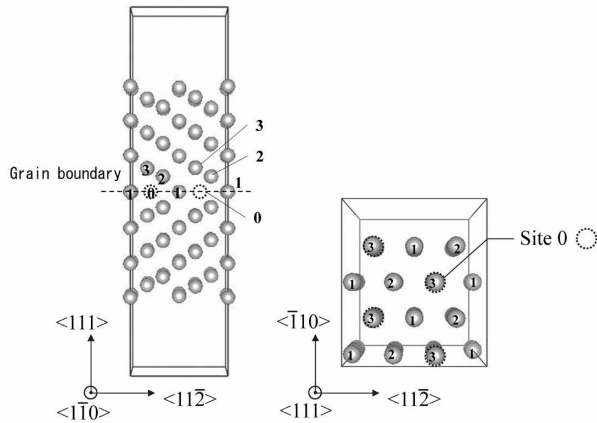


Fig. 1 bcc-Fe $\Sigma 3(111)$ grain boundary model

grain boundary. This result suggests that the grain boundary segregation tendency at the $\Sigma 3$ grain boundary also applies to other random grain boundaries.

The grain boundary segregation sites have been numbered from 0 to 3, as shown in the figure, and the additive elements P, Cr, Mn, and Mo have been arranged at these sites. In the co-segregation calculations, the sites 0 to 3 have been occupied, respectively, by either P or a transition metal element X (here, X refers to one of the elements, Cr, Mn, or Mo), and the calculations have been carried out for a total of $4 \times 4 = 16$ arrangements. Since the grain boundary segregation energy of the additive elements corresponds to the energy difference between the time when they are segregated on grain boundaries and when they are dissolved as a solid solution in the grains, it has been calculated from Eq.(1):

$$E_{\text{seg}}^{\text{gb}}[X] = E_{\text{gb}}[\text{Fe-X}] + E_{\text{bk}}[\text{Fe}] - \{E_{\text{gb}}[\text{Fe}] + E_{\text{bk}}[\text{Fe-X}] + \mu_{\text{Fe}}\} \quad \dots \dots \dots (1)$$

wherein $E_{\text{gb}}[\text{Fe-X}]$, $E_{\text{bk}}[\text{Fe-X}]$, $E_{\text{bk}}[\text{Fe}]$, and $E_{\text{gb}}[\text{Fe}]$ respectively represent the Fe grain boundary when an X atom segregates to a grain boundary, iron crystals when X atom is dissolved as a solid solution in a grain, pure iron crystal, and the total grain boundary energy of pure iron Fe. μ_{Fe} is a chemical potential term for correcting the number of Fe atoms.

The P-X interatomic interaction energy, $E_{\text{int}}[\text{P}, \text{X}]$, and the grain boundary co-segregation energy, $E_{\text{coseg}}[\text{P}, \text{X}]$, when P and X atoms co-segregate, are defined by Equations (2) and (3), respectively:

$$E_{\text{int}}[\text{P}, \text{X}] = E_{\text{gb}}[\text{Fe-P-X}] + E_{\text{gb}}[\text{Fe}] - \{E_{\text{gb}}[\text{Fe-P}] + E_{\text{gb}}[\text{Fe-X}]\} \quad \dots \dots \dots (2)$$

$$E_{\text{coseg}}[\text{P}, \text{X}] = E_{\text{gb}}[\text{Fe-P-X}] + 2E_{\text{bk}}[\text{Fe}] - \{E_{\text{gb}}[\text{Fe}] + E_{\text{bk}}[\text{Fe-P}] + E_{\text{bk}}[\text{Fe-X}]\} \quad \dots \dots \dots (3)$$

wherein $E_{\text{gb}}[\text{Fe-P-X}]$ is the total energy of the Fe grain boundary when P and X atoms are arranged at the grain boundary, and $E_{\text{int}}[\text{P}, \text{X}]$ is the energy difference between the time when the P and X atoms are co-segregated at a grain boundary and when they are independently segregated. $E_{\text{coseg}}[\text{P}, \text{X}]$ is the energy difference between the time when the P and X atoms co-segregate at the grain boundary and the time when they are solid-solutioned in the grain, and the P and X atomic arrangements that minimize $E_{\text{coseg}}[\text{P}, \text{X}]$ are the most likely ones.

The grain boundary binding energy corresponds to the grain boundary strength and is expressed by Eq. (4) using grain boundary energy, surface energy, and grain boundary area S:

$$E_{\text{bind}} = (2E_{\text{surf}} - E_{\text{gb}})/S \quad \dots \dots \dots (4)$$

The first-principles calculations have employed the Vienna Abinitio Simulation Package (VASP) code based on the density functional theory,¹²⁾ and the interatomic potential has used the Perdew-Burke-Ernzerhof (PBE) type Projector-Augmented-Wave (PAW) potential.¹³⁾ The cutoff energy of the plane wave basis set is 280 eV, and the k-point mesh in the grain-boundary model in Fig. 1 is $3 \times 4 \times 1$ of the Monkhorst Pack. In addition, the 0.2 eV-wide Methfessel-Paxton smearing method¹⁴⁾ has been used to improve convergence. For structure optimization calculation, all atoms are relaxed after the alloy atoms have been arranged, and the convergence condition has been set to an atomic force of 0.02 eV/Å or less.

2. Calculation results and considerations

2.1 Grain boundary segregation energy during independent segregation

In order to investigate how easily each element segregates on grain boundaries, the grain boundary segregation energy during independent segregation has been calculated for P, Cr, Mn, and Mo. The results are shown in Fig. 2 (a) to (d). The lower the value, the easier it is to segregate. Phosphorus has the lowest grain boundary segregation energy, and its segregation energies are -1.0 eV/atom and -1.15 eV / atom at Site 0 and Site 2, respectively. Similar to P, Site 2 is most stable for Cr and Mn, and their segregation energies are -0.19 eV/atom and -0.32 eV/atom, respectively. Of the elements, Mo is the only one most stable at Site 1, and its segregation energy is -0.41 eV/atom.

On grain boundaries, the atomic arrangement is different from that in grains. Therefore, the Voronoi volume, which corresponds to the volume of the

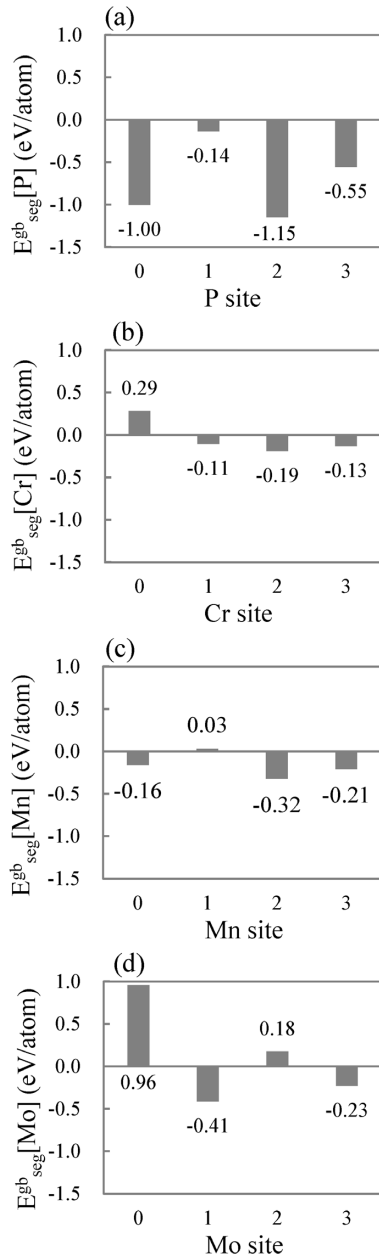


Fig. 2 Calculation results of grain boundary segregation energy at Fe grain boundary ((a)P, (b)Cr, (c)Mn, (d) Mo)

space occupied by one atom, differs from that in a Fe crystal grain. It is known that the grain boundary segregation energy depends strongly on the Voronoi volume.⁹⁾ Fig. 3 shows the relationship between the Voronoi volumes of the alloying elements and the segregation energies at the segregation sites. The numbers in the graph indicate the segregation site numbers. The Voronoi volumes at pure-iron grain boundaries are 10.2, 13.1, 11.1, and 12.3 Å³ at Sites 0, 1, 2, and 3, respectively.

The elements P, Cr, and Mn with Voronoi volumes of 11.1 to 11.3 Å³ in iron crystal grains are most stable at Site 2, while Mo with a Voronoi volume of 11.7 Å³ is most stable at Site 1. Each tends

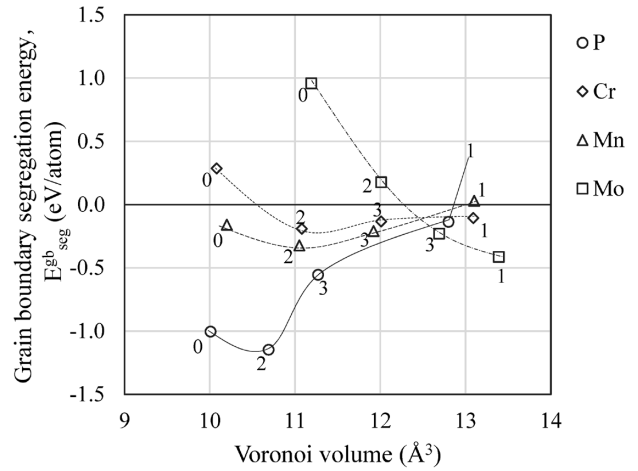


Fig. 3 Relationship between grain boundary segregation energy and Voronoi volume

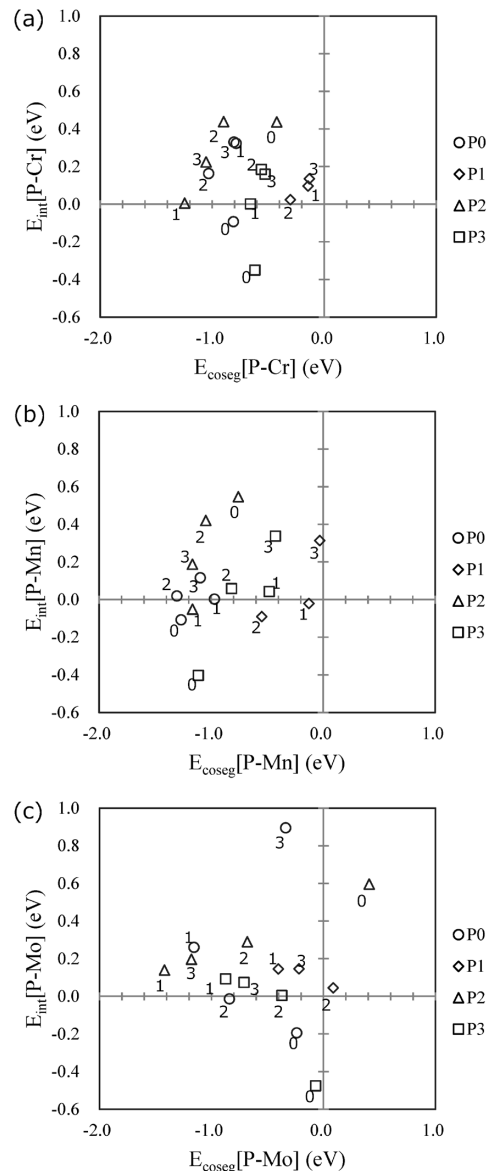


Fig. 4 Relationship between co-segregation energy and interaction energy with P and X[X=(a)Cr, (b)Mn, (c) Mo] atoms at Fe grain boundary

to enter a site at the grain boundary with a Voronoi volume similar to itself. In particular, P and Mo, each having an atomic radius significantly different from the base material Fe, are more stable when put on grain boundaries, where various atomic volumes are allowed to exist, and the grain boundary segregation energy decreases.

2.2 Grain boundary segregation energy during co-segregation

Next, P and X are arranged simultaneously on the grain boundary to investigate the P-X interaction energy and co-segregation energy on grain boundaries for each atomic arrangement. The results are shown in Fig. 4 (a) to (c). The plots in (a) to (c) indicate the atomic arrangement of P, and the numbers in the figure are the site numbers of the X atom. The lower the co-segregation energy on the horizontal axis, the higher the feasibility of the atomic arrangement in the grain boundary co-segregation. The element P with a low energy of independent segregation tends to have low co-segregation energy when arranged at Site 0 or Site 2. Many plots fall in the first quadrant of the graph, where the interaction energy is positive, and as a whole, repulsive interaction works with P. The interaction energy varies widely from -0.5 to +1.0 eV/atom, and the arrangement of P and X atoms is considered to have a significant effect. As for the differences among the elemental species, Mn has negative interaction energy for P0-Mn0 (arrangement of P and Mn to Site 0, respectively)

and for arrangement P3-Mn0, which has low co-segregation energy, and its repulsive interaction is weaker than those of Cr and Mo.

Similarly, as a result of calculating the P-X interatomic interaction in the bcc-Fe crystal grain from the first-principles calculations, the interaction energies of Cr, Mn, and Mo against P are -0.06, -0.24, and +0.02, respectively. Since Mn has an attractive interaction with P in the crystal and the repulsive interaction is weaker than those of Cr and Mo, this tendency is considered to be inherited even at the grain boundary.

2.3 Dependence of grain boundary segregation energy on Voronoi volume

Fig. 5 (a) to (f) show the results of investigating the relationship between the grain boundary segregation energy of P-X atoms during co-segregation and the Voronoi volume. Fig. 5 (a) and (d), (b) and (e), and (c) and (f) are the results of the co-segregation of P and X atoms, respectively. The upper figures (a) to (c) show the relationship between the segregation energy and Voronoi volume for the P atoms, while the lower figures (d) to (f) show those for the X atoms. The solid plots indicate the relationship during independent segregation, and the numerical values in the figures indicate the sites of coupling atoms. As for P, the grain boundary segregation energy depends on the Voronoi volume of P, although there are variations, and, as in the case of independent segregation, this energy tends to have a minimum value of around 10.5 to 11.0 Å³

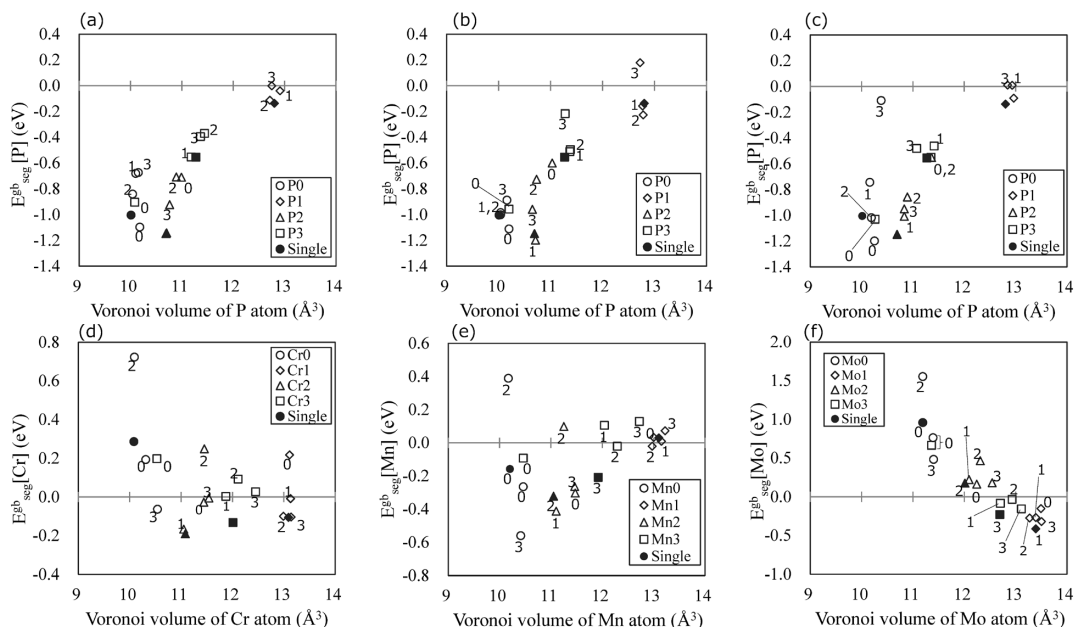


Fig. 5 Relationship between grain boundary segregation energy and Voronoi volume of segregation atoms during P, X co-segregation. (X=Cr (a, d), Mn (b, e), Mo (c, f))

during co-segregation. On the other hand, Cr and Mn do not show as significant a Voronoi volume dependence as that of P and are considered to be strongly influenced by the interaction with P.

Now the effect of atomic position is studied in detail. From Fig. 5 (a) to (c), when P is arranged at Site 0 (notation P0 in the figure), the Voronoi volume increases due to the arrangement of X atoms at P0-X0, so the grain boundary segregation energy of P becomes lower than that during independent segregation. On the other hand, in P0-X1 and P0-X2, the segregation energy of P tends to increase slightly, and in P0-X3, the segregation energy of P increases significantly in the case of Cr and Mo.

Fig. 6 (a) and (b) show the grain boundary structures of the P0-X1 and P0-X3 arrangement, respectively. The interatomic distance of P0-X1 is 2.52 to 2.57 Å, while that of P0-X3 is 2.21 to 2.31 Å, the latter being shorter than the former. The nearest distance of P, X atoms neighboring in Fe grains is 2.49 to 2.58 Å, and the P0-X3 arrangement is shorter than this. Therefore, the P atom is subjected to a considerable strain, generating a significant repulsive force. This effect is particularly significant for Mo, which has a large atomic radius. The same is true when P is arranged on Site 2, where the interatomic distance of P2-X1 is 2.57 to 2.76 Å, whereas P2-X2 is as small as 2.2 to 2.35 Å; in the latter case, the segregation energy of P is increased.

Fig. 7 shows the relationship between P-X

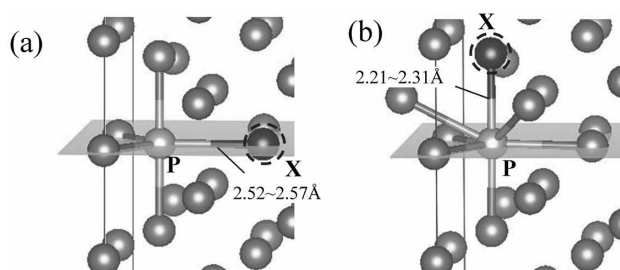


Fig. 6 Grain boundary structure in case of (a)P0-X1 and (b)P0-X3 atomic configuration

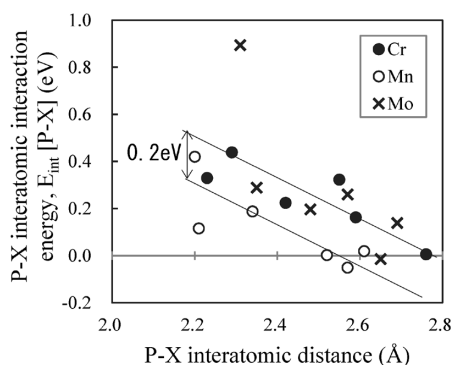


Fig. 7 Relationship between P-X interatomic interaction energy and interatomic distance on grain boundary

interatomic interaction energy and the interatomic distance when P is arranged at Sites 0 and 2. This result indicates that the repulsive force is more significant near 2.2 Å, where the interatomic distance is short, and the interaction energy becomes zero at around 2.6 Å for Mn and 2.8 Å for Cr and Mo. Thus, the interaction energy correlates with the P-X interatomic distance, and as shown in Fig. 7, Cr and Mo have a repulsive interaction stronger than that of Mn by approximately 0.2 eV.

2.4 Effect of grain boundary segregation elements on grain boundary strengthening and embrittlement

Changes in grain boundary binding energy have been calculated to investigate the effect of alloying elements on the grain boundary strength, and the results are shown in Table 1. Since the grain boundary binding energy depends on the difference between the surface segregation energy and the grain boundary segregation energy, these energies are also described. Element P has a surface segregation energy lower than the grain boundary segregation energy (surface segregation is increasingly stable). Therefore, the sign of grain boundary binding energy is negative, and as is known empirically, it causes grain boundary embrittlement. On the other hand, Cr, Mn, and Mo all show positive values and have a grain boundary strengthening effect, in which Mo is prone to grain boundary segregation and has the most significant strengthening effect. Generally, elements prone to grain boundary segregation have a low surface segregation energy like P, but this does not apply to Mo, which shows a positive sign.

In order to investigate the effect of surface segregation energy, the differential charge density distribution during surface segregation (change in charge density due to the arrangement of P and Mo on the surface) has been analyzed. The results are shown in Fig. 8. The differential charge density is caused by the fact that the P and Mo arranged on the surface are bound to 4 Fe atoms on the bulk side

Table 1 Surface segregation energies, grain boundary segregation energies, and grain boundary binding energies of P, Cr, Mn, and Mo

Atom	E_{seg}^{sf} (eV/atom)	E_{seg}^{gb} (eV/atom)	ΔE_{bind}^{gb} (J/m ²)
P	-1.50	-1.15	-0.10
Cr	-0.09	-0.19	0.03
Mn	-0.02	-0.32	0.09
Mo	0.11	-0.41	0.15

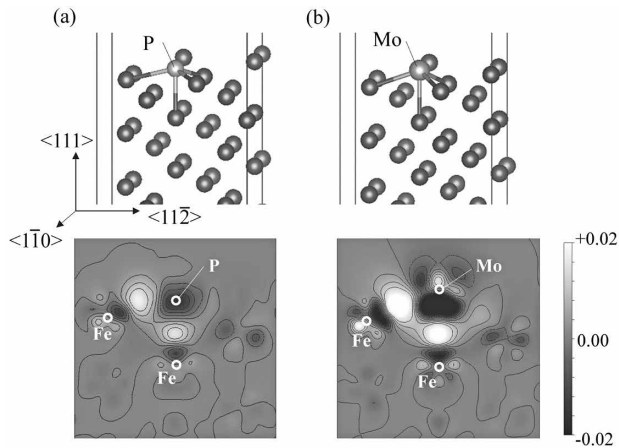


Fig. 8 Fe(111) surface structure and differential charge density distribution during (a)P and (b)Mo segregation

but are unbonded on the surface side. Mo exhibits a differential charge density in this part, while P does not. This difference is attributed to the fact that, in P, 3s and 3p electrons create a valence band, whereas Mo constitutes a valence band with 4d electrons. The d electrons have a narrower bandwidth than the s or p electrons and have an electron cloud that is more strongly anisotropic. Therefore, the repulsing electrons are also distributed on the side of unstable unbonded hands, resulting in the high surface segregation energy.

Conclusions

The first-principles calculations have been used to consider the effects of the transition metal elements, Cr, Mn, and Mo, on the grain boundary segregation of P at the Fe Σ 3 (111) grain boundary from the perspective of grain boundary interaction. It has been shown that all of the elements exhibit the grain boundary segregation tendency, and the grain boundary segregation energy depends on the

relationship between the Voronoi volume and the atomic radius of the segregation site.

The elements Cr, Mn, and Mo, show repulsive interaction with P on grain boundaries and are expected to reduce the grain-boundary segregation of P from the viewpoint of interatomic interaction. It was also found that, among the three elements, Mo is expected to increase the grain boundary binding energy by grain boundary segregation and suppress the grain boundary embrittlement by P.

On the other hand, in actual materials, it is necessary to consider various phenomena such as the formation of grain boundary characters and grain boundary precipitates, carbide formation, which affects the segregation amount, and the change in the solid-solution amount due to the formation of precipitates. It is considered that the future challenge will be to predict the segregation amount after examining these effects in more detail.

References

- 1) Y. Murakami et al. Bulletin of the Japan Institute of Metals. 1981, Vol.20, No.9, pp.784-793.
- 2) J. Murakami et al. Tetsu- to-Hagane. 1987, Vol.73, No.1, pp.191-198.
- 3) F. Matsuda. JOURNAL OF THE JAPAN WELDING SOCIETY. 1967, Vol.36, No.9, pp.973-986.
- 4) J. Kameda. Bulletin of the Japan Institute of Metals. 1980, Vol.19, No.8, pp.595-603.
- 5) J. Yu et al. Met. Trans. A. 1980, Vol.11A, pp.291-300.
- 6) J. Wu et al. Mat. Charact. 2008, Vol.59, pp.261-265.
- 7) M. Carcia-Mazario. J. Nuc. Mat. 2007, Vol.360, pp.293-303.
- 8) M. Yamaguchi. J. Japan Inst. Met. Mater. 2008, Vol.72, No.9, pp.657-666.
- 9) J. Wang et al. Acta. Mat. 2016, Vol.115, pp.259-268.
- 10) Y-J. Hu et al. Comp. Mat. Sci. 2020, Vol.171, p.109271.
- 11) E. Nakajima et al. Tetsu-to-Hagane. 2000, Vol.86, No.5, pp.357-362.
- 12) G. Kresse et al. Phys. Rev. B. 1994, Vol.49, pp.14251-14269.
- 13) G. Kresse et al. Phys. Rev. B. 1999, Vol.59, pp.1758-1775.
- 14) M. Methfessel et al. Phys. Rev. B. 1989, Vol.40, pp.3616-3621.